ARMA 11-420

Undrained Plane Strain Compression of Shale

Makhnenko, R.Y., Riedel, J.J. and Labuz, J.F.
University of Minnesota, Minneapolis, MN, USA

This paper was prepared for presentation at the 45th US Rock Mechanics / Geomechanics Symposium held in San Francisco, CA, June 26–29, 2011.

ABSTRACT: Pierre shale was tested under an undrained condition within the University of Minnesota Plane-Strain Apparatus, which was modified to allow application and measurement of pore pressure. A rectangular, prismatic specimen was carefully machined and assembled with porous stones between the upper and lower steel platens; the specimen, porous stones, and platens were held together with a custom jig and a thin layer of polyurethane was applied to prevent confining fluid from penetrating the shale. Once air was removed from the system, equal back pressure was applied to the top and bottom of the specimen. The back pressure was incrementally (1 MPa) increased to 8 MPa, and held constant for ten days, with confining pressure 0.35 MPa higher than back pressure. The maximum *B*-value achieved was 0.63. The undrained, plane strain compression test was performed with an initial confining stress of 4 MPa, and an average lateral displacement rate of 10^{-4} mm/s; peak stress was reached in about one hour. Measurements of axial and lateral displacements, axial load, confining and pore pressures provided the necessary information to calculate the undrained and drained elastic parameters of the rock within the framework of poroelasticity.

1. INTRODUCTION

The presence of pore fluids can affect the deformation process and facilitate or delay material failure [1]. Dilation of rock in undrained deformation induces a reduction of pore pressure and growth of the limit stress value [2]. On the other hand, a contractive response induces an increase of pore pressure and reduction of the failure stress [3].

For undrained deformation processes with the condition of isochoric deformation (vanishing rate of volumetric strain), the limit surfaces are reached for lower shear stress values than those for drained deformation. Further, depending on the material density and initial pressure, there can be several limit states with adjacent domains of stability and instability [1].

The overall project concerns the testing of water-saturated soft rock such as shale under plane-strain compression, where drained properties are difficult to determine because of low permeability. Dilatant hardening and contractant softening will be investigated from undrained experiments, where pore pressure will be measured throughout the deformation process. This paper presents the results of an undrained, plane strain experiment on Pierre shale. Poroelastic parameters of the rock were calculated from measurements of axial and lateral displacements, axial load, confining and pore pressures. Values of porosity, Skempton (*B*-value) coefficient, and bulk modulus of the fluid used for saturation were estimated prior to compression testing. Poroelastic theory introduced by Biot [4,5] and developed by Rice and Cleary [6] and Detournay and Cheng [7] was used to determine the undrained and drained elastic parameters.

2. BACKGROUND

2.1. Plane-Strain Apparatus

An apparatus for determining the constitutive response of soft rock, named the University of Minnesota Plane-Strain Apparatus, was designed and built based on a passive stiff-frame concept [8]. The biaxial device (U.S. Patent 5,063,785) is unique because it allows the failure plane to develop and propagate in an unrestricted manner. By placing the upper platen on a low friction linear bearing, the prismatic specimen, subjected to confining pressure and compressed axially, has the freedom to translate in the lateral direction if the deformation has localized. In addition, the apparatus was modified to allow pore pressure to be applied and monitored during an experiment.

The design of the Plane-Strain Apparatus is illustrated in Fig. 1; a brief explanation of the various parts of the device follows. A prismatic specimen (1) of height 75-100 mm, thickness 30-40 mm, and width 100 mm, is covered with an impermeable polyurethane coating to

isolate the rock from the confining fluid. The specimen is placed on a lower loading platen (2) and confined laterally by a biaxial frame (3) in the form of a thick-walled cylinder. A pair of equally angled wedges allowing a tolerance of 0.5 mm in specimen width is used for fitting the specimen within the biaxial frame (Fig. 2). The lower loading plate is connected through a load cell (4) to the base unit (5) of the apparatus. The biaxial frame sits on the base unit guided by three pins, which ensures precise alignment. Another loading plate (6) rests on top of the specimen; it is fixed with bolts to a linear bearing (7) sliding over a trackway (8). The trackway is connected through bolts to a loading piston (9). The apparatus is placed inside a large pressure cell to induce confining (lateral) stress. The cell consists of a base pot (10), a pressure vessel (11) rated to 24 MPa, and an upper cap (12). Low friction teflon O-rings are used for sealing the loading piston and the upper caps, as well as the other connecting members of the pressure cell. The cell is filled with hydraulic oil and the confining pressure is applied with a microprocessor-based hydraulic pump that maintains cell pressure at a constant value, within a tolerance of 0.15 MPa.

The apparatus is internally instrumented with LVDTs for determining lateral and axial displacements of the specimen and movement of the linear bearing, a load cell for measuring the axial force, and strain gages for estimating the deformation of the biaxial frame. The confining pressure is recorded by a pressure transducer within the hydraulic system. Two pressure transducers record the pore pressure both at the bottom and top of the specimen.

The axial force is measured below and above the specimen. A 1 MN load cell, with a sensitivity of 50 kN/mV, is mounted permanently to the cross head of the load frame and provides the axial force above the specimen. A confining pressure-compensated load cell, with a sensitivity of 5 kN/mV, is placed below the specimen, between the lower loading platen and the base unit.

Five RDP-Electrosense type D5/100/90, pressure resistant LVDTs with a linear range of 2.5 mm and a sensitivity of 0.25 mm/mV measure the displacements of the specimen and the linear bearing. Two LVDTs are attached to the upper loading platen for measuring axial displacement. A pair of LVDTs are placed horizontally on opposite sides of the specimen exposed to confining pressure at 5 mm above and below the specimen's mid-height for measuring lateral displacement. The four LVDTs are mounted in place through LVDT holders attached with two aluminum posts to the lower loading platen (Fig. 1). One LVDT is attached to the linear bearing to record its horizontal displacement.

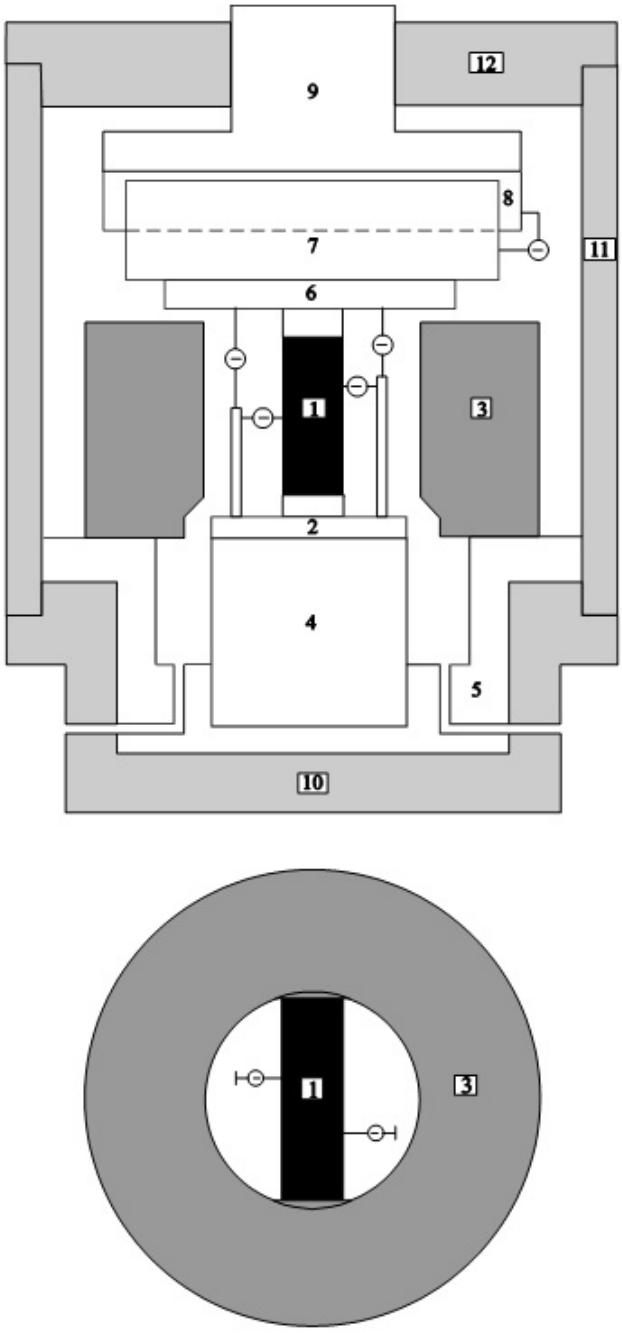

Fig. 1. University of Minnesota Plane-Strain Apparatus.

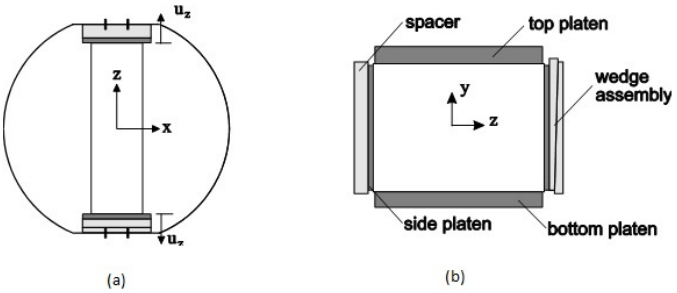

Fig. 2. Specimen and wedge-spacer assembly. a. Plan view. b. Elevation view.

2.2. *Drained and Undrained Plane-Strain Elastic Parameters*

Generalized Hooke's law for the incremental behavior of an isotropic linearly elastic solid in plane-strain takes the following form for principal strains and stresses (ε_2=0):

$$\Delta\varepsilon_1 = \frac{1+\nu}{E}\left[(1-\nu)\Delta\sigma_1 - \nu\Delta\sigma_3\right]$$
$$\Delta\varepsilon_3 = \frac{1+\nu}{E}\left[(1-\nu)\Delta\sigma_3 - \nu\Delta\sigma_1\right] \quad (1)$$
$$\Delta\sigma_2 = \nu\left(\Delta\sigma_1 + \Delta\sigma_3\right)$$

Assuming constant confining pressure throughout the test ($\Delta\sigma_3$=0) and taking the sign convention of compression positive, Young's modulus E and Poisson's ratio ν are

$$E = \Delta\sigma_1 \frac{\Delta\varepsilon_1 - 2\Delta\varepsilon_3}{\left(\Delta\varepsilon_1 - \Delta\varepsilon_3\right)^2} \quad (2)$$

$$\nu = \frac{-\Delta\varepsilon_3}{\Delta\varepsilon_1 - \Delta\varepsilon_3} \quad (3)$$

For plane problems, it is convenient to introduce the invariants named (i) mean stress s, (ii) shear stress t, (iii) volume strain ε_V, and (iv) shear strain γ:

$$s = \left(\sigma_1 + \sigma_3\right)/2$$
$$t = \left(\sigma_1 - \sigma_3\right)/2 \quad (4)$$
$$\varepsilon_V = \varepsilon_1 + \varepsilon_3$$
$$\gamma = \varepsilon_1 - \varepsilon_3$$

Generalized Hooke's law for plane-strain becomes

$$\Delta\gamma = \frac{1}{G}\Delta t \quad (5)$$

$$\Delta\varepsilon_V = \frac{2(1+\nu)}{3K}\Delta s \quad (6)$$

Bulk modulus K and shear modulus G are

$$K = \frac{E}{3(1-2\nu)} \quad (7)$$

$$G = \frac{E}{2(1+\nu)} \quad (8)$$

For undrained elastic behavior in terms of total stresses, undrained Young's modulus E_u and undrained Poisson's ratio ν_u are introduced. Then, generalized Hooke's law for undrained plane-strain loading can be written in terms of equations (5) and (6), but for undrained elastic parameters:

$$\Delta\varepsilon_V = \frac{2(1+\nu_u)}{3K_u}\Delta s \quad (9)$$

$$\Delta\gamma_u = \frac{1}{G_u}\Delta t \quad (10)$$

where undrained bulk and shear moduli are

$$K_u = \frac{E_u}{3(1-2\nu_u)} \quad (11)$$

$$G_u = \frac{E_u}{2(1+\nu_u)} \quad (12)$$

In case of undrained testing, the pore pressure u must be considered and effective stresses take the following form:

$$\sigma_1' = \sigma_1 - u$$
$$\sigma_3' = \sigma_3 - u \quad (13)$$
$$s' = \left(\sigma_1' + \sigma_3'\right)/2$$
$$t' = \left(\sigma_1' - \sigma_3'\right)/2 = \left(\sigma_1 - \sigma_3\right)/2 = t$$

Furthermore, because $\Delta t' = \Delta t$,

$$G_u = G' \quad (14)$$

where G' is the drained shear modulus, which will be denoted as G for convenience.

Therefore, once ν_u and E_u are obtained from an undrained plane-strain test, other parameters such as K_u and G can be determined. Moreover, knowing values of the Skempton coefficient B, porosity of the rock ϕ, and the bulk modulus of the fluid used for saturation K_f, the following equations are associated with the poroelastic response [7]:

$$\alpha = 1 - \frac{K}{K_s'}$$
$$K_u = K + \frac{\alpha^2 K}{(1-\alpha)\alpha + \phi K\left(\frac{1}{K_f} - \frac{1}{K_s''}\right)} \quad (15)$$
$$B = \frac{\alpha}{\alpha + \phi K\left(\frac{1}{K_f} - \frac{1}{K_s''}\right)}$$

The coefficients K_s' and K_s'' are two bulk moduli, which under certain conditions can be both identified with the bulk modulus K_s of the solid constituent. Assuming that the rock does not have nonconnected pore space, all points of the solid phase may be taken as elastically isotropic with the same local bulk modulus K_s, and both fluid and solid are chemically inert for the time scale of the tests (a few weeks), it can be shown that [7]

$$K_s = K_s' = K_s'' \quad (16)$$

The interstitial water of a nearly saturated (S > 90%) soil is a mixture of water and gas that has a fluid bulk modulus K_f [9]:

$$\frac{1}{K_f} = \frac{1}{K_w} + \frac{1-S}{p} \quad (17)$$

where p is the absolute pressure in the fluid, S is the degree of saturation, and K_w=2.2GPa is the bulk modulus of pure water [10]. Equation (17) shows that even a small variation in the degree of saturation strongly influences the bulk modulus of the fluid.

Equations (15) can be solved for K and K_s, and the following inequalities must be satisfied [7]:

$$0 < K < K_u \tag{18}$$

$$0 < K < K_s \tag{19}$$

Knowing K and G, the drained Poisson's ratio $\nu' = \nu$ is

$$\nu = \frac{3K - 2G}{2(3K + G)} \tag{20}$$

Also, drained Young's modulus $E' = E$ can be calculated in terms of drained Poisson's ratio ν and shear modulus G from equation (7).

In summary, for rock where drained testing for some reason may not be possible, values of K, K_s, ν, and E can be estimated from the parameters calculated from undrained plane-strain tests: G, K_u, and B, assuming that rock porosity ϕ and the bulk modulus of the fluid K_f are known.

3. EXPERIMENTAL PROCEDURE

3.1. Specimen Preparation

The experiment was conducted on Pierre shale sample with porosity ϕ=0.40 and dry bulk density 1.6 g/cm^3. Mineralogical composition of Pierre shale varies depending on where the specimens are obtained [11]: carbonate 10-15%, quartz+feldspar 20-30%, illite 15-30%, montmorillonite 10-15%, and kaolinite 10-20%, with traces of pyrite; the tested sample had >50% clay minerals. The permeability of the shale is very low and varies form 1-14 nD [12] to 200-500 nD [13].

A Pierre shale specimen was cut from a 200 mm diameter core so that the major principal stress was applied perpendicular to bedding. The specimen dimensions were 100 x 44 x 86 mm (Fig. 3). All of the faces of the specimen were cut such that opposite sides were parallel and adjacent sides were perpendicular within ±0.05 mm in 100 mm.

The specimen was assembled with porous stones between the upper and lower steel platens; the porous stones were in contact with the 100 x 44 mm faces of the specimen. Two steel plates, 3 mm thick, contacted the 44 x 86 mm faces (Fig. 2). Two circular (10-mm diameter) brass buttons 1-mm thick were glued to the specimen to provide a firm contact for the probes of the lateral LVDTs. The specimen, porous stones, and platens were held together with a custom jig and a thin layer of polyurethane was applied to the 100 x 86 mm faces over a thin rubber membrane. The polyurethane prevented confining fluid from penetrating the specimen. The specimen and platen assembly were placed within the biaxial frame and prestressed with the proper wedge and spacer combination.

Figure 3. Specimen of Pierre shale prior to testing.

3.2. Test procedure

The pore pressure system within the apparatus was designed so that pressure could be applied to the bottom of the specimen while the top of the specimen was left open to atmospheric pressure; this allowed water to be flushed through the shale. The pore pressure system was also capable of applying equal pore pressure on the bottom and top of the specimen.

The technique of applying back pressure to the pore water is commonly used in testing of fine-grained soil and rock. The purpose of back pressure is to saturate the specimen by dissolving any gas present in the pore water. Increase of the pore pressure in a partially saturated specimen affects the volume of the gas in the pores in two ways: (1) by direct compression, the gas is reduced in volume according to Boyle's law; (2) by application of a higher pressure, additional amounts of gas are dissolved in the pore water in accordance with Henry's law of solubility [14].

Back pressure of 1.4 MPa was applied to the bottom of the specimen while the top of the specimen was opened to the atmosphere, releasing excess air, as the pore water permeated through the specimen. During this phase of the test the confining pressure was 0.7 MPa higher than the pore pressure that was applied to the bottom of the specimen. This was done to avoid harmful swelling of the shale when water was forced into the specimen [15].

Once the air was removed from the system, equal back pressure was applied to the top and bottom of the specimen. The back pressure was then incrementally (1 MPa) increased to 8 MPa and held constant for 10 days. The confining pressure was 0.35 MPa higher than the back pressure.

The Skempton coefficient B is given by

$$B = \Delta u / \Delta \sigma_3 \qquad (21)$$

From equations (15), B = 1 can be achieved only when the confining fluid is much stiffer than the skeleton, which is often the case for soil. The very low permeability makes shale a very special material to study: fluid-saturated testing becomes extremely time-consuming, since pore pressure equilibration is slow. After ten days of back pressure, the maximum B-value achieved for the specimen was 0.63; because of time constraints, it was decided to conduct the deviatoric loading phase through plane strain compression.

The cell pressure was increased to 12 MPa for an initial σ_3=4 MPa, and the specimen was allowed to consolidate for four days. The plane strain compression test was performed with a lateral displacement rate of 10^{-4} mm/s. Peak stress was attained in about one hour. Load, cell pressure, pore pressure, axial displacement, lateral displacement, and sled displacement were measured.

4. EXPERIMENTAL RESULTS

The results of the plane-strain compression test are presented as axial force - axial displacement (Fig. 4), lateral displacements - axial displacement (Fig. 5), shear stress - shear strain (Fig. 6), and pore pressure - shear strain (Fig. 7). The initial linear regions of Figs. 4 and 6 were used to calculate the undrained elastic parameters from equations (2), (3), (5) and (11):

$E_u = 270MPa$, $\nu_u = 0.37$ and

$K_u = 340MPa$, $G = 100MPa$.

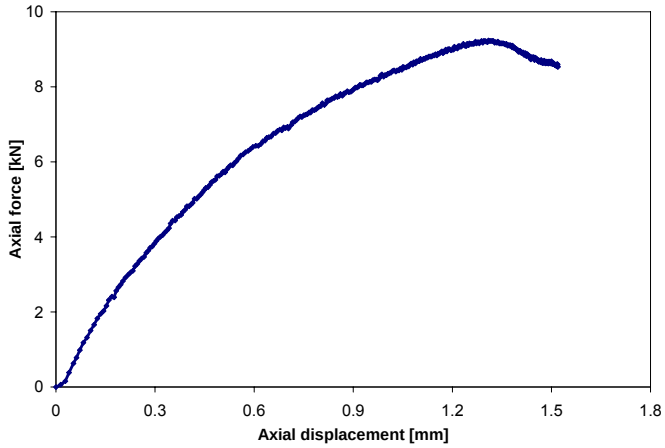

Fig. 4. Undrained mechanical response of the shale.

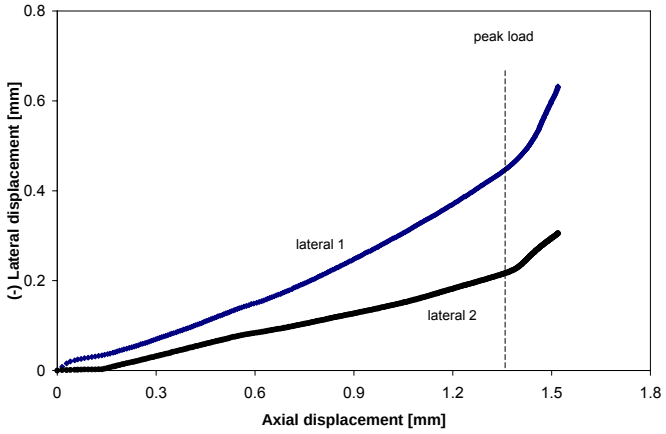

Fig. 5. Deformation response of the shale, pre- and post-peak.

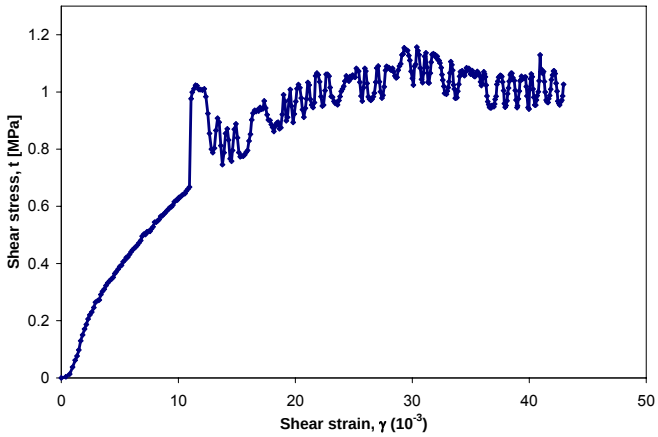

Fig. 6. Deviatoric response of the shale for undrained loading.

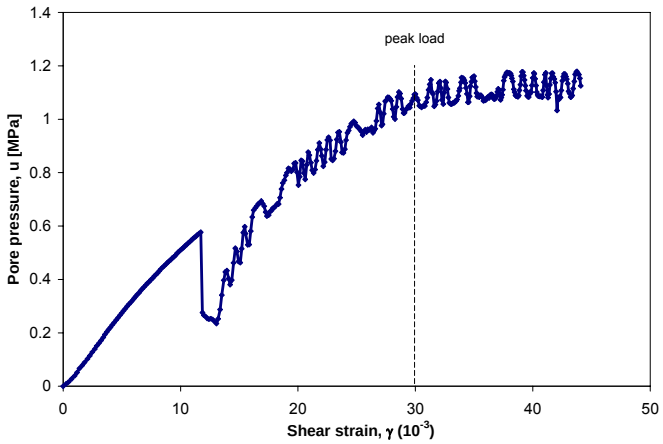

Fig. 7. Pore pressure response of the shale.

The specimen exhibited a peak axial load, followed by a softening response (Fig. 4). At the end of the experiment, the failed Pierre shale specimen was removed from the biaxial frame, and no visible shear band was detected.

The behavior of the two lateral LVDTs shown in Fig. 5 indicates that the deformation of the specimen was not uniform, as the slopes in the pre-peak regions should be

parallel. In addition, the rate of deformation increased after peak load, even though no localization was visible after the test.

An abrupt increase in shear stress (Fig. 6) and decrease in pore pressure (Fig. 7) at the value of shear strain γ=0.011 were due to a momentary uncontrolled decrease in cell pressure. Note that $t = f(-\sigma_3)$, and a decrease in σ_3 will cause a decrease in pore pressure, as described by equation (21). Furthermore, fluctuations in the t and u during compression beyond γ=0.011 were also related to the precision of the control system for the cell pressure σ_3. Nevertheless, at peak shear stress, the shear strain γ=0.03, and the pore pressure remained approximately constant in the post-peak region.

If the specimen was assumed to be fully saturated (S=1), $K_f = 2.2GPa$ from equation (17), and then K and K_s from equations (15) would be negative. Thus, even with ten days of back pressure saturation, the specimen was not fully saturated (S<1), which is in an agreement with the discussion on difficulties in attaining 100% saturation of low permeable rock [14].

Inequalities (18) and (19) are satisfied only for S≤0.97. Knowing that pressure in the fluid p=7.8MPa before the test was started, K_f was calculated from equation (17), and then used in equations (15) to calculate the bulk modulus K and the bulk modulus of solid constituent K_s. Young's modulus and drained Poisson's ratio are obtained from equations (20) and (7).

Assuming a value of S=0.97, K_f=230MPa and the material parameters are

$K = 260MPa$, $\alpha = 0.27$, and $K_s = 360MPa$,

$E = 260MPa$ and $\nu = 0.33$.

If S=0.93, K_f=106MPa and the material parameters are

$K = 150MPa$, $\alpha = 0.85$, and $K_s = 990MPa$,

$E = 240MPa$ and $\nu = 0.23$.

The latter result is in agreement with hydrostatic consolidation tests on Pierre shale described by Savage and Braddock [16]. They obtained K=124MPa and H=143MPa for the direction perpendicular to the bedding of the rock at hydrostatic stress equal to 5MPa. Here H characterizes the coupling between the solid strain and pore pressure and is related to α [7]:

$$\alpha = \frac{K}{H} \qquad (22)$$

which gives α=0.87 and K_s=950MPa, close to the values obtained from the plain strain tests assuming S=0.93. Moreover, the results of true triaxial tests described in [17] provide values of E=220MPa and ν=0.31 for the direction of loading perpendicular to the bedding plane, which is also in agreement with the reported values.

It is important to note that values of undrained Young's modulus E_u and undrained Poisson's ratio v_u are very sensitive to the accuracy of axial and lateral displacement measurements, which are related not only to the specimen, but also to the system; *i.e.* axial and lateral displacements contain system displacements that must be removed to obtain material response. Conducting a calibration test with materials of known properties, such as aluminum or PMMA, allows both lateral and axial system displacements to be determined. For example, the measured response was a nonlinear function of the axial load < 60 kN (Fig. 8) for a calibration test conducted with an aluminum specimen with no confinement. This correction must be checked at various stress states ($\sigma_3 \neq 0$) with a material of similar to the tested rock stiffness (*e.g.* PMMA).

5. CONCLUDING REMARKS

Pierre shale was tested under an undrained condition within the University of Minnesota Plane-Strain Apparatus. Measurements of axial and lateral displacements, axial load, confining and pore pressures provided the necessary information to calculate the undrained and drained elastic parameters of the rock within the framework of isotropic poroelasticity. Future experiments will be conducted with a more permeable rock that will allow both undrained and drained loading under plane-strain compression, and the failure response of the rock will be considered.

ACKNOWLEDGEMENTS: Partial support was provided by DOE Grant DE-FE0002020 funded through the American Recovery and Reinvestment Act.

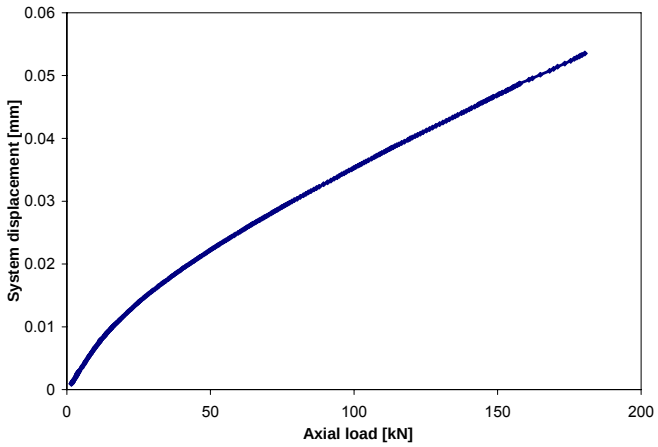

Fig. 8. Nonlinear system response.

REFERENCES

1. Mroz, Z., N. Boukpeti, A. Drescher. 2003. Constitutive model for static liquefaction. *Int. J. Geomech. ASCE.* 3: 133-144.
2. Rice, J.R. 1975. On the stability of dilatant hardening for saturated rock masses. *J. Geophys. Res.* 80(11): 1531-1536.
3. Boukpeti, N., Z. Mroz, A. Drescher. 2002. A model for static liquefaction in triaxial compression and extension. *Can. Geotech. J.* 39: 1243-1253.
4. Biot, M.A. 1941. General theory of three-dimensional consolidation. *J. Appl. Phys.* 12: 155-164.
5. Biot, M.A., D.G. Willis. 1957. The elastic coefficients of the theory of consolidation. *J. Appl. Mech.* 594-601.
6. Rice, J.R. and M.P. Cleary. 1976. Some basic stress-diffusion solutions for fluid saturated elastic porous media with compressible constituents. *Rev. Geophys. Space Phys.* 14: 227-241.
7. Detournay, E., A. Cheng. 1993. Fundamentals of poroelasticity. In *Comprehensive Rock Engineering, Vol. II,* ed. C. Fairhurst, 113-171.
8. Labuz, J.F., S.-T. Dai, and E. Papamichos. 1996. Plane-strain compression of rock-like materials. *Int. J. Rock Mech. Min. Sci.* 33(6): 573-584.
9. Verruijt, A. 1969. Elastic storage of aquifers. In *Flow through Porous Media*, ed. R.J.M. De Wiest, 331-376.
10. Bardet, J.P. and H. Sayed. 1993. Velocity and attenuation of compressional waves in nearly saturated soils. *Soil Dyn. Earthquake Eng.* 12: 391-401.
11. Schultz, L.G., H.A. Tourtelot, J.R. Gill, and J.G. Boerngen. 1980. Composition and properties of the Pierre shale and equivalent rocks, Northern Great Plains Region. *U.S. Geological Survey Prof. Paper* 1064-8.
12. Sherwood, J.D. and L. Bailey. 1994. Swelling of Shale around a Cylindrical Wellbore. *Math. and Phys. Sci.* 444: 161-184.
13. Zhou, X., Z. Zeng, and H. Liu. 2010. Laboratory testing on Pierre shale for CO_2 sequestration under clayey caprock. In *Proceedings of 44th US Rock Mechanics Symposium and 5th U.S.-Canada Rock Mechanics Symposium, Salt Lake City, 27-30 June 2010.*
14. Lowe, J. and T.C. Johnson. 1960. Use of back pressure to increase degree of saturation of triaxial test specimen. In *Conference on Shear Strength of Cohesive Soils*. 819-836.
15. Berre, T. 2011. Triaxial testing of soft rocks. *Geotech. Test. J.* 34(1): 61-75.
16. Savage, W.Z. and W.A. Braddock. 1991. A Model for hydrostatic consolidation of Pierre shale. *Int. J. Rock Mech. Min. Sci. Geomech. Abstr.* 28(5): 345-354
17. Swolfs H.S. and T.C. Nichols, Jr. 1987. Anisotropic characterization of Pierre shale – preliminary results. *U.S. Geological Survey Open file report* 87-417.